

Effect of Boundary Conditions on the Distribution of Mode I Fracture Toughness along Delamination Front in CFRP Laminates with General Fiber Orientation

Sylwester SAMBORSKI
*Department of Applied Mechanics
Lublin University of Technology
Nadbystrzycka 36 St., 20-618 Lublin, Poland
s.samborski@pollub.pl*

Received (24 January 2015)
Revised (26 February 2016)
Accepted (21 March 2016)

The paper deals with numerical analysis of the DCB test configuration together with the data reduction scheme described in the ASTM D 5528 Standard for determination of the mode I fracture toughness in case of the laminated composites with mechanical couplings. The numerical analysis based on the FEM approach was performed with the Abaqus software exploiting the VCCT technique. The results show, that the distribution of the Strain Energy Release Rate can be asymmetric and that mode mixity can occur. A need for mode separation procedures and appropriate data reduction schemes has been revealed.

Keywords: laminated composite, mechanical coupling, fracture toughness, double cantilever beam.

1. Introduction

The laminated structures made of Carbon Fiber Reinforced Polymer (CFRP) are nowadays broadly applied for machine construction, especially transportation equipment – airplanes, ships, cars, bike frames etc. This yields from a very attractive strength-to-mass density ratio compared to classical engineering materials, as well as a possibility of tailoring the mechanical properties of laminated composites. So far there has been a tendency to use the uncoupled CFRP laminates, as their mechanical behavior was simple and easy to foresee. Only recently some authors have indicated a broad and unexplored domain of mechanically coupled laminates with many advantages from the property design point of view [1, 2]. On the other hand, the discussed composites are prone to damage induced both during manufacturing and maintenance, that can be dangerous for the structure health and safety. The author of the current paper is engaged in research on laminated composite profiles

loaded in compression [3–5] in which different types of defects were observed in critical and post-critical state, as well. The experiments have revealed that delamination was the type of damage that dominated and was the one of the crucial meaning for structures' load bearing capacity. This has led to a separate branch of the above mentioned study concentrated on the influence of the general ply layup with possible different mechanical couplings and the boundary conditions on the actual distribution of mode I fracture toughness along delamination front. Such an analysis will be helpful in appropriate planning of the experimental tests such as the Double Cantilever Beam (DCB) test having in target determination of the G_{Ic} material constant for different ply angle interfaces.

The computational tool widely used in crack onset and propagation analysis is the Virtual Crack Closure Technique (VCCT) introduced by Rybicki and Kanninen [6]. This algorithm is available in the commercial Finite Element (FE) software environment ABAQUS [7] in which a series of laminated general layup models were built and analyzed towards delamination onset and propagation.

2. Mechanical couplings in CFRP laminates

The Classical Lamination Theory (CLT) provides relations among a laminated structure's strains/curvatures and the resulting forces/moments [1, 2]. The constitutive relations take the following compact form:

$$\begin{Bmatrix} N \\ M \end{Bmatrix} = \begin{Bmatrix} A & B \\ B & D \end{Bmatrix} \quad (1)$$

The stiffness matrices are defined as follows:

- the extensional stiffness matrix:

$$A_{ij} = \sum_{k=1}^n (\bar{Q}_{ij})_k t_k \quad (2)$$

- the coupling stiffness matrix:

$$B_{ij} = \sum_{k=1}^n (\bar{Q}_{ij})_k t_k z_k^c \quad (3)$$

- bending stiffness matrix:

$$D_{ij} = \sum_{k=1}^n (\bar{Q}_{ij})_k \left(t_k (z_k^c)^2 + \frac{t_k^3}{12} \right) \quad (4)$$

Here $(\bar{Q}_{ij})_k$ stand for the elements of the k -th ply stiffness matrix; t_k and z_k^c are the k -th ply thickness and its center-point coordinate, respectively. Note, that different forms of the matrices A, B and D describe a set of possible mechanical couplings [1, 2].

3. Methodology of numerical analysis

The VCCT technique [6, 8, 9] is based on Linear Elastic Fracture Mechanics (LEFM) and as such can be applied to composites when the nonlinearities are negligible [10]. In the current article delamination is assumed to be placed between still the same two layers and not to propagate across the plies. This assumption is justified by the aim of the research, which is recognition of the effect of coupling on the local circumstances for delamination onset.

The beam model was composed of two parts (the upper and the bottom) stucked together along ca. 2/3 of the total beam length using a proper bonding formulation in accordance with the VCCT demands. The free ends of the beam could separate freely, as allowed by the boundary conditions (BCs). However, for the sake of numerical model definition correctness the appropriate contact formulation was applied.

The current study tries to verify the practical applicability of the DCB test configuration in case of the non-UD laminates. The DCB test is based on the beam theory or the compliance calibration method, as described in the ASTM 5528-D Standard [12]. It fulfills the assumptions of the LEFM. The elaborated numerical models of the laminated beam conform with the CLT. The performed numerical analyses, based on the VCCT have shown possible discrepancies in the direct application of the ASTM 5528-D indications. Namely, the mode I Strain Energy Release Ratio (SERR, G_I) distribution along the delamination front can take different and above all asymmetric shape depending on the type of mechanical coupling and the overall layup configuration.

For the current study a bending-twisting (B-T) case of coupling has been chosen, as the one of the principal meaning in the DCB test configuration and compared with another case of a bending-extension (B-E) coupling, having however a bit less influence on the quality of the standardized DCB test results. The sequence of maximal B-T coupling, coded by York [2] as $\mathbf{A}_S\mathbf{B}_0\mathbf{D}_F$ was $[\alpha/0/\alpha/\alpha/0/-\alpha/0/-\alpha/-\alpha/-\alpha/0/-\alpha/\alpha/0/0/\alpha/\alpha]$. The latter case (B-E) marked $\mathbf{A}_S\mathbf{B}_I\mathbf{D}_S$ was composed as follows: $[\alpha/-\alpha/0/-\alpha/0/\alpha/90/\alpha/-\alpha]$. The exemplary values of the coupling matrices for a chosen fiber orientation angle $\alpha = 60^\circ$ have been collected in Table 1. Note, that the considered fiber angles were $\alpha = 0^\circ$ (UD), 30° , 45° , 60° , 90° and the layup applied to each branch of the specimen. Table 2 collects the material data used in the FE simulations. The numerical models were composed of the *Shell* type S4R finite elements and the Benzeggagh-Kennane (B-K) fracture criterion [7] was used together with the VCCT technique.

4. Results and discussion

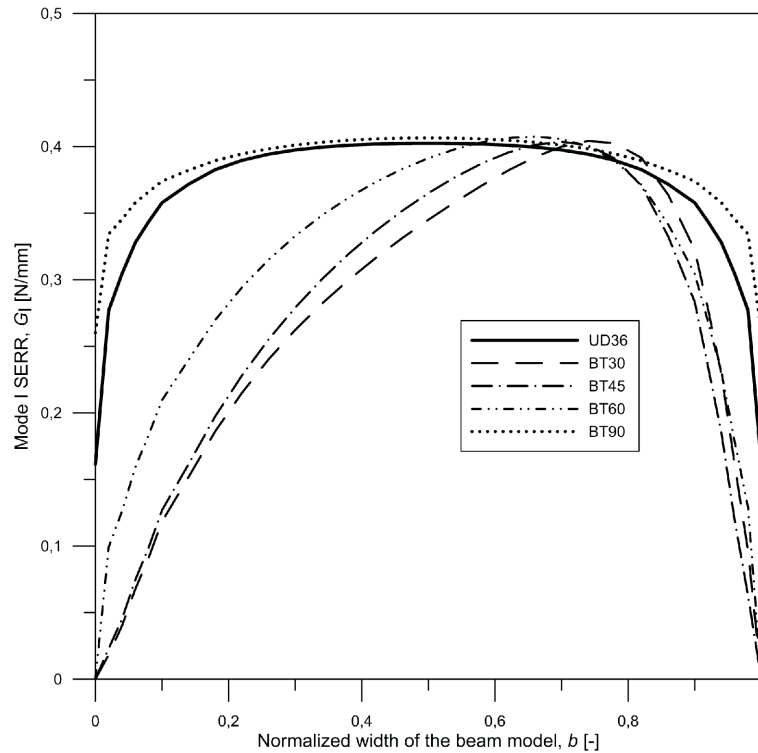
The widthwise distributions of the mode I SERR have been plotted with the G_I values calculated for the FE nodes located along delamination front at the very moment of propagation onset. As shown in Fig. 1, G_I can change significantly along the beam model width. In case of the UD composite layup (fibers along the beam's length) the plot of G_I is symmetrical and rather flat. Nevertheless, at free edges of the beam model G_I decreases. This effect is assigned in the ASTM 5528-D

Table 1 Values of the coupling matrices' components for the 60° B-T and B-E coupled laminates

Coupling matrices' terms								
A [MPa·mm]			B [MPa·mm ²]			C [MPa·mm ³]		
B-T: $\mathbf{A}_S \mathbf{B}_0 \mathbf{D}_F$ [60/0/60/60/0/-60/0/-60/-60/-60/0/60/60/0/0/60/60]								
171080	53980	0	0	0	0	184770	58300	24390
53980	171080	0	0	0	0	58300	184770	68100
0	0	58550	0	0	0	24390	68100	63240
B-E: $\mathbf{A}_S \mathbf{B}_i \mathbf{D}_S$ [60/-60/0/-60/0/60/90/60/-60]								
65310	26990	0	-8091	0	0	10790	9008	0
26990	105770	0	0	8091	0	9008	31961	0
0	0	29280	0	0	0	0	0	9625

Table 2 Composite material data used in FE simulations [11]

E_1 [GPa]	E_2 [GPa]	ν_{12}	G_{12} [GPa]	G_{Ic} [N/mm]
109.00	88.19	0.342	4.32	0.4

**Figure 1** Mode I SERR variability along the width of the B-T coupled laminate beam model

Standard to an anticlastic deformation of a beam in bending. In other words, the mode I delamination scheme induced globally through the DCB test configuration may not be fulfilled across the whole width of the beam – a mixed mode can take place (cf. [9]). The more a thorough analysis of G_I variability along delamination front should thus be performed in case of non-UD laminated beams, especially when couplings take place. For the considered bending–twisting (B–T) coupling (see the paragraph 3 for the layup sequence details) at moderate fiber orientation angles ($\alpha = 30^\circ, 45^\circ, 60^\circ$) the mode I SERR plot is much more narrow than the one for the UD beam composed of 36 plies. Moreover, it's no longer symmetric. This evokes questions on a proper data reduction scheme having in target obtaining reasonable values of mode I fracture toughness (critical SERR) – G_{Ic-ini} . The BT90 beam model seems to provide even more flat distribution of G_I widthwise, than the UD36 configuration. The explanation for this effect is that numerous layers with the 90° fiber orientation angle stiffen the beam against anticlastic effect. Note, that the B–T configuration applies to each of the DCB branches – two sets of 18 plies in one beam.

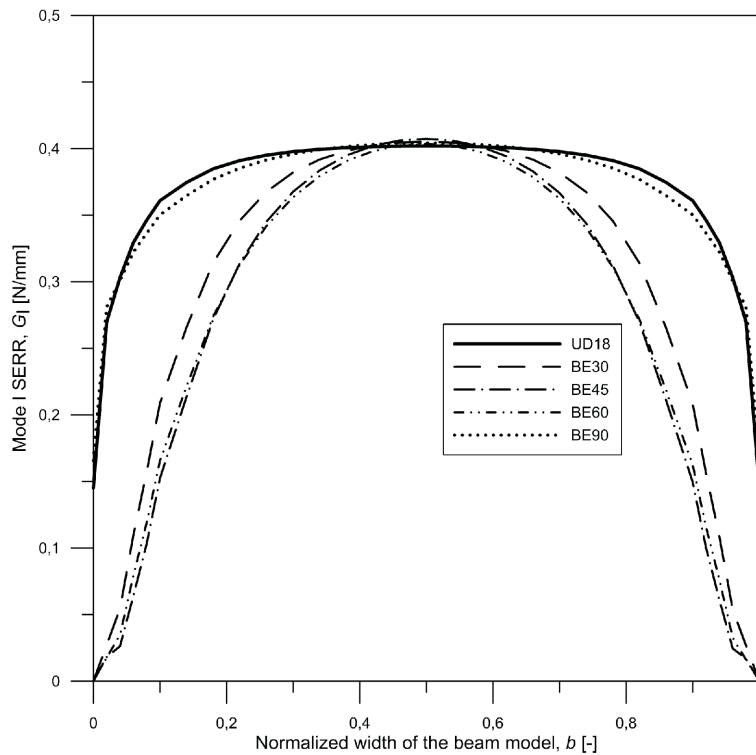


Figure 2 Mode I SERR variability along the width of the B-E coupled laminate beam model

The B–E model results shown in Fig. 2 exhibit symmetry with respect to the beam’s longitudinal axis. Nevertheless, the distribution of G_I for the moderate fiber angles remains narrow. In this case the number of plies in each branch was 9, what resulted from the requirements of the bending – extension coupling configuration. Thus, the unidirectional reference beam was composed of 18 plies in total. Distribution of the SERR for the beams UD18 and BE90 was practically the same in this case. Compared to Fig. 1, the symmetry of the plots is intrinsically related to the type of coupling: for the bending–twisting effect a tendency of the branches to rotate is the reason for the asymmetry. In both cases fracture modes different than mode I – mode II, mode III and mixed modes can be expected, as pointed out by some researchers (eg. [8, 9]). This demands a proper procedures for mode separation, which is difficult or even impossible to be attained experimentally, but relatively easy in FE codes implementing the VCCT [6, 8, 9].

5. Conclusions

The critical analysis of the DCB test configuration and the data reduction scheme applicability for the mechanically coupled laminated composite beams was performed. It revealed possible problems in the interpretation of the test results because of the non–symmetric distribution of the Strain Energy Release Rate in mode I (G_I) along the beam specimen’s width. The analysis showed the possibility of local discrepancies in the mode mixity along delamination front that could falsify the initiation values, $G_{Ic-init}$ of mode I fracture toughness, calculated in principle for the whole beam’s width. The obtained results can lead to a more reasonable planning of the experiments, especially the ply sequences and the stiffness of the loading grips. However, the key observation is that pure modes of delamination practically do not occur. Instead, mixed modes should be expected – not easy to be controlled in the experiment, in the sense of a proper data reduction scheme. Numerical methods, such as the VCCT–enhanced FEM are useful, precise and enable implementation of many fracture criteria, both for single and mixed fracture modes.

Acknowledgements

This paper was financially supported by the Ministerial Research Project No. DEC-2013/11/B/ST8/04358 financed by the Polish National Science Centre.

References

- [1] **York, C. B.:** Unified Approach to the Characterization of Coupled Composite Laminates, Benchmark Configurations and Special Cases, *J. Aerosp. Eng.*, 23(4), 219–242, **2010**.
- [2] **York, C. B.:** Tapered hygro–thermally curvature–stable laminates with non–standard ply orientations, *Composites, Part A*, 44, 140–148, **2013**.
- [3] **Teter, A., Dębski, H. and Samborski, S.:** On buckling collapse and failure analysis of thin–walled composite lipped–channel columns subjected to uniaxial compression, *Thin–Walled Structures*, 85, 324–331, **2014**.
- [4] **Kubiak, T., Samborski, S. and Teter, A.:** Experimental investigation of failure process in compressed channel–section GFRP laminate columns assisted with the acoustic emission method, *Comp. Str.*, 133, 921–929, **2015**.

- [5] **Dębski, H., Teter, A., Kubiak, T. and Samborski, S.:** Local buckling, post-buckling and collapse of thin-walled channel section composite columns subjected to quasi-static compression, *Comp. Str.*, 136, 593–601, **2016**.
- [6] **Rybicki, E. F. and Kanninen. M. F.:** A finite element calculation of stress intensity factors by a modified crack closure integral, *Eng. Fract. Mech.*, 9(4), 931–938, **1997**.
- [7] Abaqus/CAE User's Manual 6.11, Dassault Systèmes, **2011**.
- [8] **Zou, Z., Reid, S. R., Soden, P. D. and Li S.:** Mode separation of energy release rate for delamination in composite laminates using sublaminates, *Int. J. Sol. Struct.*, 38(15), 2597–2613, **2001**.
- [9] **Krueger, R.:** The virtual crack closure technique for modeling interlaminar failure and delamination in advanced composite materials, *Num. M. of Failure in Adv. Comp. Mat.*, 3–53, **2015**.
- [10] **Burlayenko, V. and Sadowski, T.:** FE modeling of delamination growth in interlaminar fracture specimens, *Bud. i Arch.*, 2, 95–109, **2008**.
- [11] **de Moura, M. F. S. F, Campilho, R. D. S. G. and Goncalves, J. P. M.:** Crack equivalent concept applied to the fracture characterization of bonded joints under pure mode I loading, *textitComp. Sci. Tech.*, 68, 2224–2230, **2008**.
- [12] ASTM D 5528: Standard test Method for Mode I Interlaminar Fracture Toughness of Unidirectional Fiber-Reinforced Polymer Matrix Composites. ASTM International, **2001**.

